

Solubility of Pyrazine and Its Derivatives in Supercritical Carbon Dioxide

Zhihao Shen, Dan Li, and Mark A. McHugh*

Department of Chemical and Life Science Engineering, Virginia Commonwealth University, 601 West Main Street, Richmond, Virginia 23220

Isopleths and solution densities are reported, from ≈ 25 to 100 °C and pressures to ≈ 200 bar, for mixtures of CO_2 with pyrazine, 2-methoxypyrazine, 2-acetylpyrazine, 2-methylpyrazine, and 2,3-dimethylpyrazine. These five solute + CO_2 systems exhibit type-I phase behavior with similar mixture critical pressures up to 100 °C. The Peng–Robinson equation of state, with k_{ij} equal to zero, provides a semi-quantitative representation of the data for all of the pyrazines with the exception of the 2-acetylpyrazine + CO_2 system, which required a k_{ij} of -0.100 to get a reasonable representation of the data. The data presented here further substantiates the observation that supercritical CO_2 can be used to extract pyrazines from natural materials.

Introduction

Pyrazines are important components that contribute to the flavor and aroma of many foods.^{1–3} Pyrazine compounds are also known to be present naturally in tobacco and are generally believed to contribute to roasted and nut-like flavors.⁴ Within the past decade, supercritical fluid (SCF) extraction has been used to analyze the pyrazine content^{5,6} of natural materials. Solubility data are needed to scale any SCF extraction process to industrial size. A few studies have reported on the phase behavior of pyrazine and pyrazine derivatives in SCF solvents. Yamamoto et al. reported the high-pressure phase behavior of binary mixtures of pyrazine with CO_2 , C_2H_4 , C_2H_6 , and CHF_3 at -63 to 67 °C and pressure to 300 bar.⁷ They found that the pyrazine + CO_2 system exhibits type-I phase behavior.^{8,9} Nakatani et al. reported the solid solubility of 2-aminopyrazine and 2-carboxylic acidpyrazine in CO_2 , C_2H_4 , C_2H_6 , and CHF_3 at 35 °C.¹⁰ Both of these compounds showed higher solubility in CO_2 than in C_2H_4 and C_2H_6 , and they have the highest solubility in CHF_3 likely due to the high polarity of CHF_3 .¹⁰

In the present paper, solubility and solution density data are reported for pyrazine, 2-methoxypyrazine, 2-acetylpyrazine, 2-methylpyrazine, and 2,3-dimethylpyrazine in CO_2 . Table 1 shows the structure, select physical properties, and critical properties of the pyrazines used in this study. The Peng–Robinson equation of state¹¹ (PR EOS) is used to model the experimental data obtained in this study. Steele et al.¹² report the critical temperature, critical pressure, and acentric factor for pyrazine. The Joback–Lydersen group contribution method¹³ is used to estimate the critical properties and acentric factor of 2-methoxypyrazine, 2-methylpyrazine, and 2,3-dimethylpyrazine and the critical pressure and acentric factor for 2-acetylpyrazine. Fedors method,¹³ which is most useful when the boiling point is not available, is used to estimate the critical temperature of 2-acetylpyrazine.

Experimental Section

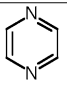
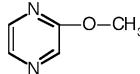
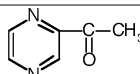
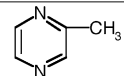
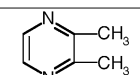
Described elsewhere are the apparatus and techniques used to obtain solute + CO_2 phase behavior data.^{14,15} The main component of the experimental apparatus is a high-pressure,

variable-volume cell (Nitronic 50, 7.0 cm o.d., 1.5 cm i.d., ≈ 15 cm^3 working volume). The empty cell is purged with CO_2 at ≈ 6 bar three times to remove traces of air. Liquid 2-methylpyrazine, 2,3-dimethylpyrazine, and 2-methoxypyrazine are then loaded into the cell to within ± 0.0001 g using a syringe. However, solid pyrazine or 2-acetylpyrazine is first loaded into the cell to within ± 0.0001 g, and the cell is then purged with CO_2 at ≈ 6 bar three times. CO_2 is then added to the cell to within ± 0.01 g using a high-pressure bomb. The solution in the cell is stirred using a stirring bar controlled by a magnet located beneath the cell. The contents of the cell are projected onto a video monitor using a camera coupled to a borescope (Olympus Corp., model F100-024-000-55) placed directly against the sapphire window. The solution temperature is measured to within ± 0.1 °C (type K thermocouple calibrated against a NIST certified thermometer) and is held constant to within ± 0.3 °C. The system pressure is measured with a Heise pressure gauge (model CM-57303) with an uncertainty of ± 1.4 bar. The mixture in the cell is compressed to a single phase, and the pressure is then slowly decreased until a second phase appears. A bubble point is obtained if small bubbles appear in the cell, a dew point is obtained if a fine mist appears in the cell, and a mixture critical point is obtained if critical opalescence is observed and if two, equal-volume phases are observed after the second phase appears. Isopleth data are averaged values from phase transition measurements reproduced 2–3 times to within ± 1.4 bar for bubble points and 2.1 bar for dew points. In both cases, the composition of the predominant phase is equal to the overall solution composition as the amount of mass present in the second phase is negligible. The solution concentrations of a given isopleth have an accumulated uncertainty of less than $\approx \pm 1\%$.

Solution density data are measured in the single-phase region up to within ± 1.4 bar of the phase transition using a linear displacement technique^{16,17} given in detail elsewhere.¹⁸ At a given pressure and temperature the volume of the cell is determined by detecting the location of the internal piston with a linear variable differential transformer coil (Lucas Schaevitz Co., model 2000-HR) that fits around a 1.43 cm high-pressure tube and tracks the magnetic tip of a steel rod connected to the piston. Solution densities are calculated knowing the amount

* Corresponding author. Fax: 804-828-3846. E-mail: mmchugh@vcu.edu.

Table 1. Structure and Physical Properties of Pyrazines Used in This Study^a

Name	Structure	Molecular Weight	$t_m/^\circ\text{C}$	$t_b/^\circ\text{C}$	$t_c/^\circ\text{C}$	P_c/bar	Acentric Factor
pyrazine		80.1	52.0	115.0	353.9	67.0	0.270
2-methoxy pyrazine		110.1	---	61.0	232.7	52.4	0.427
2-acetyl pyrazine		122.1	78.0	---	469.5	51.2	0.412
2-methyl pyrazine		94.1	-29.0	135.0	358.0	53.7	0.352
2,3-dimethyl pyrazine		108.1	12.0	156.0	374.2	45.9	0.396

^a The melting points (t_m) and boiling points (t_b) were reported by the supplier (Sigma-Aldrich Co.) with the exception of t_m of 2-methoxypyrazine, which is a liquid at room temperature. The critical temperature (t_c), the critical pressure (P_c), and the acentric factor for pyrazine were reported by Steele et al.¹² The critical temperatures for 2-methoxypyrazine, 2-methylpyrazine, and 2,3-dimethylpyrazine were calculated using the Joback–Lydersen method.¹³ The t_c for 2-acetylpyrazine was calculated with Fedors method¹³ since this method does not use the boiling point. The critical pressures and acentric factors for the substituted pyrazines were calculated using the Joback–Lydersen method.¹³

of material in the cell and the cell volume. The solution densities have an accumulated uncertainty of less than $\pm 2\%$.¹⁸

Materials. CO₂ was obtained from Roberts Oxygen Corporation (99.5 % minimum purity) and used as received. Pyrazine (99.95 % purity), 2-methylpyrazine (99.7 % purity), 2,3-dimethylpyrazine (99.9 % purity), 2-methoxypyrazine (99.9 % purity), and 2-acetylpyrazine (99.9 % purity) were obtained from Sigma-Aldrich Co. and used as received.

Results and Discussion

Tables 2 to 6 list the P , t isopleth data obtained in this study along with the density data at each phase transition for all of the systems and density data in the one-phase region for the pyrazine, 2-methylpyrazine, and 2,3-dimethylpyrazine systems. Smooth curves are fit to the P , t isopleth data that are then cross plotted to generate graphs of the pressure–composition (P , x) isotherms. The P , x plots presented here only show smoothed curves from the P , t data.

The isopleths in Figure 1 demonstrate that only modest pressures are needed to dissolve pyrazine in CO₂ even at 100 °C. Although not presented here, the isopleths for the four pyrazine derivative + CO₂ systems exhibit very similar behavior and pressures to those of the pyrazine + CO₂ system. Figure 2 shows the P , x isotherms of pyrazine, 2-methoxypyrazine, 2-acetylpyrazine, 2-methylpyrazine, and 2,3-dimethylpyrazine in CO₂ at 25, 50, 75, and 100 °C. The 25 and 50 °C pyrazine + CO₂ isotherms in Figure 2A are truncated at the solid + liquid + gas-phase boundary reported by Yamamoto et al.⁷ The 2-acetylpyrazine + CO₂ 50 °C isotherm in Figure 2C is also truncated at the highest solute mole fraction investigated where the solute-rich phase was a liquid. The 25 °C 2-acetylpyrazine + CO₂ isotherm is not shown in Figure 2C since only a few

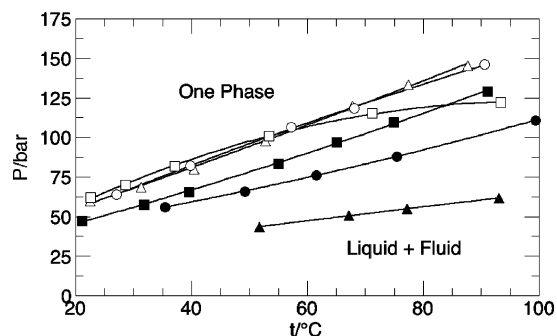


Figure 1. Isopleth data for the x pyrazine + CO₂ system obtained in this study. Only a few isopleths are shown to avoid crowding the graph. Δ , $x = 0.116$; \circ , $x = 0.056$; \square , $x = 0.028$; \blacksquare , $x = 0.308$; \bullet , $x = 0.495$; \blacktriangle , $x = 0.725$.

bubble points were obtained at 2-acetylpyrazine mole fractions less than ≈ 0.03 . Information on the solid + liquid + gas boundary for the 2-acetylpyrazine + CO₂ system is needed to define more precisely the (25 and 50) °C isotherms that should be truncated. Found elsewhere^{7,8,19} are more details on the characteristics of the global phase diagrams for solute–solvent mixtures that exhibit three-phase solid + liquid + gas behavior very near a mixture critical curve.

The shape and maximum pressures for the pyrazine isotherms at mole fractions below ≈ 0.50 (Figure 2A) are similar to those isotherms where a methyl group (Figure 2D), two methyl groups (Figure 2E), or a methoxy group (Figure 2B) is added to pyrazine. However, the (75 and 100) °C isotherms for the 2-acetylpyrazine + CO₂ system are at significantly higher pressures, which is not surprising since 2-acetylpyrazine has the highest melting point and the highest molecular weight of

Table 2. Experimental Pressure P and Density ρ at Temperature t for Pyrazine + CO₂ at Various Mole Fractions x of Pyrazine^a

t	P	ρ		t	P	ρ		t	P	ρ		t	P	ρ		t	P	ρ	
°C	bar	g·cm ⁻³		°C	bar	g·cm ⁻³		°C	bar	g·cm ⁻³		°C	bar	g·cm ⁻³		°C	bar	g·cm ⁻³	
$x = 0.015$																			
25.1	64.8	0.857	BP	25.1	65.9	0.863	S	25.1	68.6	0.873	S	25.1	75.2	0.892	S	25.1	87.9	0.918	S
30.6	72.8	0.802	BP	30.6	74.8	0.828	S	30.6	81.7	0.861	S	30.6	94.1	0.898	S	30.6	102.4	0.917	S
30.6	124.5	0.956	S	38.9	84.7	0.656	BP	38.9	89.3	0.713	S	38.9	97.6	0.778	S	38.9	99.3	0.787	S
38.9	104.1	0.812	S	38.9	111.0	0.835	S	38.9	119.0	0.856	S	45.8	89.7	0.452	DP	45.8	92.1	0.512	S
45.8	92.8	0.527	S	45.8	94.8	0.571	S	45.8	99.0	0.607	S	51.5	92.4	0.382	DP	51.5	93.4	0.394	S
51.5	96.2	0.408	S	51.5	98.3	0.423	S	51.5	104.5	0.527	S	51.5	109.7	0.576	S	51.5	113.8	0.611	S
51.5	116.2	0.627	S	51.5	117.6	0.640	S	51.5	124.5	0.674	S								
$x = 0.019$																			
22.4	61.0	0.842	BP	22.4	64.5	0.854	S	22.4	70.0	0.877	S	22.4	90.7	0.915	S	31.0	72.9	0.776	BP
31.0	76.9	0.791	S	31.0	83.8	0.826	S	31.0	92.1	0.849	S	31.0	105.2	0.876	S	31.0	119.0	0.898	S
40.5	89.0	0.679	BP	40.5	90.3	0.687	S	40.5	91.4	0.712	S	40.5	98.3	0.761	S	40.5	104.5	0.792	S
40.5	108.6	0.809	S	40.5	125.2	0.850	S	53.0	97.4	0.442	DP	53.0	99.0	0.460	S	53.0	105.2	0.580	S
53.0	111.4	0.656	S	53.0	115.2	0.688	S	53.0	123.1	0.729	S	65.3	110.7	0.431	DP	65.3	115.2	0.475	S
65.3	119.7	0.512	S	65.3	121.7	0.526	S	65.3	125.9	0.565	S	79.2	107.6	0.324	DP	79.2	111.4	0.335	S
79.2	112.1	0.352	S	79.2	123.1	0.415	S	79.2	124.8	0.428	S	79.2	127.9	0.443	S				
$x = 0.074$																			
22.5	58.3	0.922	BP	22.5	59.7	0.926	S	22.5	61.0	0.929	S	22.5	63.1	0.941	S	30.5	67.7	0.900	BP
30.5	70.7	0.903	S	30.5	87.2	0.924	S	35.1	73.8	0.878	BP	35.1	75.5	0.882	S	35.1	94.8	0.906	S
50.2	96.4	0.810	BP	50.2	100.3	0.825	S	50.2	102.4	0.835	S	50.2	119.0	0.876	S	66.3	119.7	0.695	BP
66.3	125.9	0.708	S	66.3	132.8	0.750	S	78.8	132.6	0.589	BP	78.8	134.5	0.604	S	78.8	162.8	0.719	S
93.1	147.2	0.532	BP	93.1	149.3	0.542	S	93.1	157.6	0.547	S	93.1	168.6	0.511	S				
$x = 0.090$																			
23.1	59.0	0.864	BP	23.1	61.4	0.873	S	23.1	98.3	0.923	S	32.7	70.5	0.854	BP	32.7	73.4	0.858	S
32.7	101.7	0.884	S	42.7	83.8	0.810	BP	42.7	86.6	0.813	S	42.7	86.6	0.813	S	47.0	90.3	0.799	BP
47.0	91.4	0.806	S	47.0	107.9	0.830	S	64.7	117.1	0.727	BP	64.7	121.7	0.738	S	64.7	125.9	0.752	S
64.7	159.0	0.815	S	75.8	132.8	0.672	BP	75.8	133.8	0.684	S	75.8	136.9	0.683	S	75.8	164.5	0.771	S
92.5	149.0	0.582	BP	92.5	152.1	0.591	S												
$x = 0.116$																			
22.5	59.7	0.809	BP	22.5	63.8	0.815	S	22.5	82.1	0.833	S	31.1	68.5	0.795	BP	31.1	73.4	0.798	S
31.1	75.5	0.801	S	31.1	95.5	0.816	S	40.4	79.8	0.771	BP	40.4	84.5	0.773	S	40.4	87.9	0.778	S
40.4	108.6	0.791	S	52.7	97.9	0.734	BP	52.7	101.7	0.739	S	52.7	131.4	0.767	S	67.8	120.0	0.684	BP
67.8	123.8	0.693	S	67.8	152.1	0.739	S	77.4	133.2	0.651	BP	77.4	137.6	0.665	S	77.4	155.2	0.707	S
87.7	145.4	0.620	BP	87.7	148.6	0.630	S	87.7	177.2	0.695	S								
$x = 0.146$																			
22.5	54.9	0.887	BP	22.5	55.2	0.887	S	22.5	65.2	0.898	S	22.5	127.9	0.926	S	32.6	66.7	0.860	BP
32.6	69.3	0.862	S	32.6	72.8	0.863	S	32.6	116.9	0.886	S	41.7	78.3	0.830	BP	41.7	82.4	0.833	S
41.7	88.6	0.839	S	41.7	142.4	0.869	S	54.1	96.6	0.970	BP	54.1	101.7	0.980	S	54.1	159.0	0.990	S
63.9	110.7	0.753	BP	63.9	116.6	0.760	S	63.9	151.4	0.792	S	77.7	131.2	0.703	BP	77.7	134.1	0.708	S
$x = 0.177$																			
27.6	60.5	0.889	BP	27.6	65.2	0.894	S	27.6	70.7	0.898	S	27.6	107.9	0.917	S	36.3	69.8	0.870	BP
36.3	70.7	0.872	S	36.3	76.2	0.874	S	36.3	97.6	0.884	S	48.4	85.9	0.834	BP	48.4	92.8	0.839	S
48.4	105.2	0.847	S	48.4	125.2	0.857	S	48.4	145.9	0.866	S	60.9	103.8	0.795	BP	60.9	115.5	0.803	S
60.9	119.0	0.809	S	60.9	155.9	0.831	S	74.6	123.8	0.751	BP	74.6	130.3	0.758	S	74.6	141.0	0.770	S
74.6	167.9	0.792	S	89.1	144.5	0.704	BP	89.1	147.2	0.709	S	89.1	148.3	0.712	S	89.1	194.8	0.761	S
$x = 0.224$																			
26.3	58.6	0.910	BP	26.3	77.6	0.921	S	38.9	71.9	0.887	BP	38.9	94.8	0.899	S	38.9	167.9	0.919	S
47.8	82.8	0.870	BP	47.8	96.6	0.877	S	47.8	130.0	0.889	S	59.8	100.0	0.842	BP	59.8	180.3	0.879	S
71.9	116.6	0.816	BP	71.9	124.5	0.823	S	71.9	193.4	0.858	S	89.2	141.5	0.770	BP	89.2	146.6	0.779	S
89.2	186.6	0.802	S																
$x = 0.308$																			
21.1	47.2	1.048	BP	21.1	53.4	1.054	S	21.1	94.8	1.070	S	21.1	121.7	1.078	S	31.8	57.4	1.028	BP
31.8	72.8	1.036	S	31.8	96.9	1.041	S	31.8	136.2	1.052	S	39.6	65.4	1.019	BP	39.6	77.6	1.023	S
39.6	116.9	1.033	S	39.6	148.3	1.043	S	55.0	96.9	0.970	BP	55.0	118.3	0.980	S	55.0	137.6	0.990	S
55.0	153.4	0.997	S	74.9	109.7	0.957	BP	74.9	123.1	0.965	S	74.9	176.2	0.986	S	74.9	197.2	0.996	S
91.1	129.1	*	BP																
$x = 0.397$																			
33.2	56.0	1.042	BP	33.2	65.2	1.049	S	33.2	96.9	1.061	S	33.2	136.9	1.070	S	41.8	63.6	1.037	BP
41.8	78.3	1.040	S	41.8	112.8	1.048	S	41.8	151.4	1.060	S	53.5	75.2	1.017	BP	53.5	88.6	1.023	S
53.5	110.7	1.027	S	53.5	141.0	1.036	S	72.4	95.9	0.991	BP	72.4	103.8	0.995	S	72.4	124.8	0.999	S
72.4	128.6	1.002	S	96.5	124.8	0.952	BP	96.5	145.5	0.964	S	96.5	164.1	0.968	S	96.5	207.2	0.982	S
$x = 0.495$																			
35.5	56.0	0.992	BP	35.5	60.3	0.999	S	35.5	70.0	1.001	S	35.5	92.4	1.008	S	49.2	66.0	0.975	BP
49.2	74.1	0.980	S	49.2	103.1	0.990	S	49.2	130.0	0.963	S	61.6	76.0	0.972	BP	61.6	103.4	0.980	S
61.6	135.5	0.987	S	61.6	194.1	1.002	S	75.4	87.9	*	BP	75.4	107.9	*	S	75.4	135.5	*	S
75.4	176.9	*	S	99.4	110.9	0.955	BP	99.4	114.8	0.959	S	99.4	127.2	0.962	S	99.4	150.0	0.970	S

^a BP is bubble point. DP is dew point. S is a single phase. An asterisk (*) indicates that density data were not obtained at these conditions.

Table 3. Experimental Pressure P and Density ρ at Temperature t for 2-Methoxypyrazine + CO₂ at Various Mole Fractions x of 2-Methoxypyrazine^a

t	P	ρ		t	P	ρ		t	P	ρ	
°C	bar	g·cm ⁻³		°C	bar	g·cm ⁻³		°C	bar	g·cm ⁻³	
$x = 0.007$											
31.2	72.9	0.679	BP								
$x = 0.015$											
22.1	57.6	0.726	BP	26.4	63.8	0.749	BP	30.6	70.0	0.718	BP
41.2	87.2	0.616	DP	55.1	101.0	0.451	DP	81.2	117.9	0.340	DP
$x = 0.025$											
23.2	59.6	0.797	BP	30.2	69.3	0.778	BP	40.4	84.8	0.696	BP
55.5	105.3	0.557	DP	74.6	127.2	0.474	DP	96.4	139.3	0.393	DP
$x = 0.039$											
22.1	56.5	0.780	BP	34.8	73.1	0.778	BP	54.7	105.8	0.654	DP
77.6	134.7	0.536	DP	99.1	155.1	0.469	DP				
$x = 0.069$											
22.0	54.5	0.809	BP	34.0	70.7	0.843	BP	53.9	103.8	0.756	DP
77.6	137.7	0.641	DP	97.4	162.2	0.579	DP				
$x = 0.107$											
21.2	51.7	0.802	BP	37.5	73.4	0.860	BP	59.7	109.3	0.794	BP
80.2	140.7	0.723	DP	98.6	166.2	0.672	DP				
$x = 0.129$											
21.4	52.1	0.922	BP	34.4	67.2	0.920	BP	53.7	97.9	0.864	BP
74.7	133.5	0.798	DP	95.7	161.1	0.724	DP				
$x = 0.207$											
22.6	49.3	0.911	BP	33.8	63.1	0.945	BP	55.3	92.7	0.906	BP
75.4	126.5	0.866	DP	94.5	155.1	0.824	DP				
$x = 0.232$											
23.7	50.0	0.981	BP	41.0	70.7	0.987	BP	59.3	96.9	0.948	BP
81.0	132.4	0.902	DP	95.8	152.0	0.864	DP				
$x = 0.379$											
22.6	41.4	0.929	BP	25.0	43.8	0.934	BP	39.4	58.3	1.012	BP
57.5	76.9	0.982	DP	75.5	96.9	0.958	DP	93.3	118.6	0.933	DP
$x = 0.637$											
24.0	28.1	1.053	BP	38.8	36.9	1.122	BP	59.5	49.0	1.097	BP
81.2	63.1	1.070	DP	94.2	72.0	1.055	DP				
$x = 0.919$											
22.0	7.2	1.033	BP	24.0	9.2	1.109	BP	26.8	10.8	1.063	BP
32.8	10.0	1.097	BP	44.7	11.4	1.085	BP	59.5	12.4	1.063	BP
75.8	14.7	1.050	DP								

^a BP is bubble point. DP is dew point.

the pyrazines considered in this study. From the phase behavior shown in Figure 1 and Figure 2, panels A, B, D, and E, it is apparent that these pyrazine + CO₂ mixtures exhibit type-I phase behavior.^{8,9} Yamamoto et al.⁷ have also confirmed that the pyrazine + CO₂ system exhibits type-I phase behavior. Although it is likely that the 2-acetylpyrazine + CO₂ mixture also exhibits type-I behavior, the solidification of 2-acetylpyrazine at temperatures near the critical point of CO₂ makes it difficult to determine unequivocally that type-I behavior is exhibited.

Table 7 lists mixture critical data for the pyrazine + CO₂ system obtained in this study, and Figure 3 compares the mixture critical data obtained in this study to the data of Yamamoto et al.⁷ The mixture critical data obtained in the present study are consistently slightly greater than the data of Yamamoto et al.,⁷ although the maximum pressure difference is less than 3 bar between the data of Yamamoto et al.⁷ and those calculated from a curve fit to the data obtained in this study. It should be noted that error bars on the measured pressure for both studies are hidden by the symbols used in Figure 3. The agreement with the data of Yamamoto et al. is considered to be very good given the uncertainty in the data reported here and that reported by Yamamoto et al.⁷

Table 4. Experimental Pressure P and Density ρ at Temperature t for 2-Acetylpyrazine + CO₂ at Various Mole Fractions x of 2-Acetylpyrazine^a

t	P	ρ		t	P	ρ		t	P	ρ	
°C	bar	g·cm ⁻³		°C	bar	g·cm ⁻³		°C	bar	g·cm ⁻³	
$x = 0.007$											
21.6	58.9	0.799	BP	30.2	70.0	0.724	BP	39.6	79.6	0.601	DP
$x = 0.025$											
23.0	57.9	0.758	BP	29.2	66.5	0.790	BP	41.3	86.2	0.815	DP
67.3	135.1	0.718	DP	95.7	174.8	0.628	DP				
$x = 0.054$											
29.2	64.8	0.922	BP	37.2	78.9	0.837	BP	48.1	98.9	0.785	DP
59.7	121.3	0.739	DP	75.6	154.8	0.702	DP	98.1	191.7	0.648	DP
$x = 0.081$											
33.1	70.3	0.946	BP	40.5	82.3	0.911	BP	61.3	126.2	0.856	DP
80.4	165.8	0.807	DP	96.4	196.8	0.772	DP				
$x = 0.114$											
39.8	79.6	1.092	BP	49.9	97.6	1.061	BP	61.8	123.4	1.023	BP
75.4	158.9	0.993	DP	91.7	185.8	0.945	DP				
$x = 0.138$											
36.3	70.8	1.276	BP	41.2	77.7	1.258	BP	49.1	91.9	1.238	BP
59.6	111.3	1.216	DP	72.6	139.3	1.187	DP	89.9	178.2	1.148	DP
$x = 0.161$											
37.9	75.8	0.938	BP	48.3	94.1	0.918	BP	64.8	128.6	0.887	BP
80.6	164.1	0.863	DP	97.7	197.2	0.832	DP				
$x = 0.194$											
40.0	77.6	0.954	BP	48.8	92.7	0.939	BP	60.3	114.8	0.920	BP
78.0	151.7	0.892	DP	94.7	187.9	0.861	DP				
$x = 0.295$											
48.9	81.4	1.090	BP	60.3	98.9	1.014	BP	70.6	116.0	0.998	BP
82.9	137.2	0.979	DP	95.6	159.3	0.956	DP				
$x = 0.448$											
59.4	79.6	1.063	BP	74.9	97.2	1.037	BP	93.1	119.6	1.007	BP
$x = 0.944$											
73.2	21.7	1.013	BP	87.8	22.4	0.996	BP	97.9	24.5	0.992	BP

^a BP is bubble point. DP is dew point.

Modeling. The pyrazine + CO₂ data are modeled using the PR EOS with the following mixing rules:

$$a_{\text{mix}} = \sum_i \sum_j x_i x_j a_{ij} \quad (1)$$

$$a_{ij} = (a_{ii} a_{jj})^{0.5} (1 - k_{ij}) \quad (2)$$

$$b_{\text{mix}} = \sum_i x_i b_i \quad (3)$$

where k_{ij} is a mixture parameter that is determined by fitting P , x data, and a_{ii} and b_{ii} are pure component parameters.¹¹ Table 1 lists the pure-component critical temperatures, critical pressures, and acentric factors reported by Steele et al.¹² for pyrazine and estimated for the other pyrazines using the Joback–Lydersen method. As a check on the Joback–Lydersen method, the calculated critical conditions and acentric factor for pyrazine ($t_c = 343.4$ °C, $P_c = 63.6$ bar, and $\omega = 0.309$) are in reasonable agreement with those reported by Steele et al.¹² shown in Table 1. Phase equilibrium calculations are performed for pyrazine with the critical properties reported by Steele et al.¹² The critical temperature, critical pressure, and acentric factor for CO₂ (31.04 °C, 73.8 bar, and 0.225, respectively) are obtained from the literature.¹³

Figure 4 shows how modest changes in k_{ij} can affect the 75 °C isotherm for the pyrazine + CO₂ system. A positive value of k_{ij} increased the mole fraction of pyrazine along the bubble

Table 5. Experimental Pressure P and Density ρ at Temperature t for 2-Methylpyrazine + CO₂ at Various Mole Fractions x of 2-Methylpyrazine^a

t	P	ρ		t	P	ρ		t	P	ρ		t	P	ρ		t	P	ρ	
°C	bar	g·cm ⁻³		°C	bar	g·cm ⁻³		°C	bar	g·cm ⁻³		°C	bar	g·cm ⁻³		°C	bar	g·cm ⁻³	
$x = 0.017$																			
21.7	57.6	0.721	BP	21.7	68.3	0.749	S	21.7	89.0	0.777	S	21.7	130.0	0.821	S	36.8	81.5	0.621	BP
36.8	85.2	0.652	S	36.8	101.7	0.701	S	36.8	115.9	0.724	S	56.0	101.8	0.373	DP	56.0	104.5	0.407	S
56.0	119.3	0.574	S	56.0	131.4	0.626	S	56.0	142.4	0.652	S	67.3	109.7	0.326	DP	67.3	112.8	0.346	S
67.3	114.8	0.371	S	67.3	119.7	0.408	S	67.3	127.9	0.455	S								
$x = 0.023$																			
23.2	60.3	0.599	BP	23.2	63.1	0.607	S	23.2	66.6	0.614	S	23.2	89.3	0.642	S	28.4	67.5	0.549	BP
28.4	79.3	0.578	S	28.4	100.7	0.604	S	28.4	115.2	0.620	S	59.2	109.1	0.323	BP	59.2	112.1	0.375	S
59.2	123.4	0.438	S	59.2	132.8	0.470	S	59.2	153.4	0.519	S	59.2	166.2	0.540	S	69.2	116.2	0.279	DP
69.2	117.6	0.283	S	69.2	119.7	0.291	S	69.2	123.4	0.300	S								
$x = 0.033$																			
21.7	58.0	0.864	BP	21.7	58.6	0.869	S	21.7	77.6	0.904	S	21.7	136.9	0.969	S	38.6	84.0	0.747	BP
38.6	85.2	0.764	S	38.6	107.9	0.831	S	38.6	133.1	0.871	S	38.6	157.6	0.905	S	60.4	113.8	0.574	BP
60.4	117.9	0.617	S	60.4	127.2	0.679	S	60.4	133.4	0.719	S	60.4	153.4	0.780	S	71.5	123.0	0.468	DP
71.5	124.8	0.482	S	71.5	131.7	0.529	S	71.5	138.6	0.578	S	71.5	146.6	0.620	S	71.5	153.1	0.649	S
71.5	165.5	0.683	S	101.1	140.2	0.344	DP	101.1	140.3	0.346	S	101.1	145.5	0.367	S	101.1	150.0	0.384	S
101.1	162.4	0.425	S																
$x = 0.039$																			
25.7	62.1	0.787	BP	25.7	68.6	0.804	S	25.7	85.2	0.831	S	25.7	116.9	0.873	S	42.1	86.7	0.682	BP
42.1	96.9	0.722	S	42.1	106.9	0.749	S	42.1	126.6	0.777	S	42.1	146.6	0.812	S	53.5	104.3	0.595	BP
53.5	116.2	0.667	S	53.5	122.8	0.690	S	53.5	136.2	0.725	S	73.0	126.2	0.462	BP	73.0	143.8	0.582	S
73.0	150.7	0.617	S	79.6	131.0	0.429	DP	79.6	141.4	0.495	S	79.6	147.9	0.525	S	79.6	154.1	0.543	S
103.2	145.4	0.349	DP	103.2	148.6	0.367	S	103.2	157.6	0.406	S								
$x = 0.051$																			
21.8	55.2	*	BP	21.8	56.9	*	S	21.8	72.1	*	S	40.1	78.7	*	BP	40.1	87.9	*	S
40.1	99.7	*	S	40.1	123.8	*	S	57.2	104.9	*	BP	57.2	106.6	*	S	57.2	113.4	*	S
57.2	130.7	*	S	71.5	124.1	*	BP	71.5	132.1	*	S	71.5	140.3	*	S	97.9	152.3	*	DP
97.9	152.4	*	S	97.9	163.8	*	S	97.9	181.0	*	S								
$x = 0.062$																			
24.1	56.9	0.845	BP	24.1	57.9	0.854	S	24.1	75.5	0.873	S	24.1	95.5	0.894	S	24.1	128.3	0.914	S
42.3	83.4	0.766	BP	42.3	86.2	0.781	S	42.3	112.1	0.824	S	42.3	131.7	0.846	S	42.3	163.1	0.879	S
63.8	117.8	0.689	BP	63.8	123.4	0.716	S	63.8	132.8	0.743	S	63.8	145.2	0.775	S	63.8	169.7	0.820	S
76.6	136.4	0.660	BP	76.6	141.0	0.691	S	76.6	151.0	0.722	S	101.6	154.9	0.554	DP	101.6	161.0	0.592	S
101.6	167.2	0.626	S	101.6	169.7	0.639	S												
$x = 0.081$																			
22.7	54.6	0.779	BP	22.7	71.4	0.779	S	22.7	97.6	0.781	S	22.7	131.7	0.781	S	57.9	103.8	0.785	BP
57.9	104.5	0.785	S	57.9	105.9	0.785	S	65.4	116.0	0.746	BP	65.4	122.4	0.752	S	65.4	132.1	0.765	S
65.4	149.3	0.774	S	78.0	131.7	0.772	DP	78.0	139.7	0.778	S	78.0	147.2	0.780	S	78.0	167.2	0.783	S
101.4	157.4	0.684	DP	101.4	172.1	0.740	S	101.4	192.1	0.768	S								
$x = 0.091$																			
31.3	64.9	0.901	BP	31.3	71.4	0.913	S	31.3	86.6	0.927	S	31.3	101.7	0.940	S	44.4	84.5	0.841	BP
44.4	112.8	0.882	S	44.4	145.5	0.913	S	44.4	165.2	0.930	S	54.2	100.8	0.794	BP	54.2	107.9	0.808	S
54.2	115.2	0.822	S	54.2	133.4	0.848	S	54.2	158.3	0.875	S	68.4	123.6	0.731	BP	68.4	144.1	0.782	S
68.4	154.1	0.801	S	68.4	173.4	0.828	S	85.1	146.9	0.656	BP	85.1	156.9	0.696	S	85.1	164.5	0.714	S
85.1	176.9	0.743	S	85.1	192.1	0.767	S	85.1	206.9	0.787	S	96.0	154.8	0.618	DP	96.0	159.7	0.633	S
96.0	166.6	0.659	S	96.0	173.4	0.681	S	96.0	181.0	0.701	S	96.0	190.0	0.721	S	106.3	164.3	0.565	DP
106.3	174.1	0.598	S	106.3	203.4	0.675	S	106.3	219.0	0.705	S	106.3	242.1	0.731	S				
$x = 0.122$																			
22.4	52.6	0.947	BP	22.4	67.9	0.998	S	22.4	87.9	1.010	S	22.4	105.9	1.019	S	22.4	144.1	1.036	S
31.3	62.6	0.954	BP	31.3	78.3	0.970	S	31.3	106.6	0.989	S	31.3	136.9	1.006	S	36.0	68.4	0.934	BP
36.0	80.7	0.948	S	36.0	111.4	0.972	S	36.0	147.2	0.992	S	47.6	86.1	0.890	BP	47.6	103.4	0.910	S
47.6	117.6	0.924	S	47.6	143.8	0.944	S	59.3	104.8	0.840	BP	59.3	120.0	0.863	S	59.3	135.5	0.881	S
59.3	155.9	0.901	S	76.3	133.0	0.770	BP	76.3	141.0	0.787	S	76.3	155.2	0.810	S	76.3	163.1	0.824	S
76.3	187.9	0.852	S	92.5	155.2	0.707	BP	92.5	170.0	0.746	S	92.5	181.0	0.769	S	92.5	191.7	0.786	S
$x = 0.156$																			
22.2	50.0	0.906	BP	22.2	53.1	0.908	S	22.2	76.2	0.910	S	22.2	96.2	0.911	S	31.0	59.3	0.901	BP
31.0	67.9	0.795	S	31.0	80.3	0.905	S	31.0	102.1	0.906	S	31.0	122.1	0.911	S	44.7	77.1	0.885	BP
44.7	85.2	0.887	S	44.7	111.4	0.898	S	44.7	123.1	0.899	S	55.6	94.3	0.868	BP	55.6	99.0	0.872	S
55.6	110.0	0.878	S	55.6	139.0	0.890	S	66.1	109.2	0.843	BP	66.1	109.3	0.847	S	66.1	137.6	0.869	S
66.1	172.1	0.884	S	82.0	134.0	0.799	BP	82.0	136.9	0.808	S	82.0	145.9	0.821	S	82.0	169.3	0.843	S
102.4	163.0	0.745	BP	102.4	167.9	0.765	S	102.4	181.0	0.789	S	102.4	199.7	0.811	S				
$x = 0.264$																			
22.3	46.6	0.883	BP	22.3	54.5	0.901	S	22.3	79.0	0.911	S	22.3	124.5	0.926	S	22.3	165.9	0.934	S
31.4	55.5	0.881	BP	31.4	56.9	0.882	S	31.4	66.6	0.885	S	31.4	103.8	0.896	S	31.4	136.2	0.907	S
44.8	70.7	0.856	BP	44.8	73.4	0.858	S	44.8	90.0	0.863	S	44.8	118.3	0.872	S	44.8	154.1	0.882	S
62.5	94.0	0.822	BP	62.5	94.8	0.822	S	62.5	109.0	0.829	S	62.5	143.8	0.842	S	62.5	177.2	0.852	S
71.9	107.6	0.808	BP	71.9	107.9	0.808	S	71.9	127.2	0.818	S	71.9	152.8	0.828	S	71.9	191.7	0.842	S
102.6	156.3	0.746	BP	102.6	170.0	0.758	S	102.6	207.2	0.778	S	102.6	245.9	0.797	S				

Table 5 (Continued)

t	P	ρ		t	P	ρ		t	P	ρ		t	P	ρ		t	P	ρ	
°C	bar	g·cm ⁻³		°C	bar	g·cm ⁻³		°C	bar	g·cm ⁻³		°C	bar	g·cm ⁻³		°C	bar	g·cm ⁻³	
$x = 0.339$																			
23.0	40.3	0.928	BP	23.0	75.9	0.964	S	23.0	105.5	0.969	S	23.0	161.0	0.976	S	34.3	50.1	0.937	BP
34.3	83.4	0.950	S	34.3	112.8	0.957	S	34.3	161.7	0.965	S	52.0	68.3	0.929	BP	52.0	70.0	0.932	S
52.0	105.9	0.941	S	52.0	152.8	0.952	S	71.8	91.7	0.913	BP	71.8	113.4	0.920	S	71.8	187.2	0.941	S
81.9	104.5	0.914	BP	81.9	110.3	0.918	S	81.9	146.6	0.927	S	81.9	172.8	0.939	S	114.2	144.3	0.891	BP
114.2	154.8	0.899	S	114.2	180.7	0.912	S	114.2	227.9	0.933	S								
$x = 0.624$																			
21.9	29.3	0.944	BP	21.9	39.0	0.948	S	21.9	70.0	0.952	S	21.9	96.6	0.956	S	21.9	147.6	0.965	S
31.9	33.8	0.919	BP	31.9	36.2	0.922	S	31.9	50.0	0.926	S	31.9	74.8	0.931	S	31.9	108.6	0.937	S
31.9	154.8	0.942	S	43.3	39.8	0.907	BP	43.3	60.3	0.912	S	43.3	100.3	0.917	S	43.3	132.1	0.920	S
43.3	172.8	0.926	S	58.5	47.8	0.892	BP	58.5	63.8	0.896	S	58.5	99.0	0.901	S	58.5	134.8	0.904	S
58.5	182.4	0.910	S	75.5	57.8	0.875	BP	75.5	75.9	0.879	S	75.5	118.3	0.884	S	75.5	162.4	0.890	S
103.5	76.3	0.845	BP	103.5	79.7	0.846	S	103.5	109.7	0.852	S	103.5	149.3	0.859	S	103.5	193.4	0.864	S
$x = 0.857$																			
21.8	19.8	0.930	BP	21.8	24.5	0.935	S	21.8	37.9	0.942	S	21.8	68.6	0.947	S	21.8	115.2	0.950	S
34.4	20.7	0.916	BP	34.4	27.2	0.922	S	34.4	49.0	0.926	S	34.4	68.6	0.928	S	34.4	115.5	0.934	S
49.8	23.3	0.900	BP	49.8	47.6	0.905	S	49.8	85.2	0.909	S	49.8	126.2	0.914	S	49.8	170.3	0.918	S
63.9	25.5	0.888	BP	63.9	36.2	0.892	S	63.9	55.5	0.893	S	63.9	90.0	0.897	S	63.9	135.9	0.901	S
78.2	28.6	0.878	BP	78.2	37.6	0.878	S	78.2	70.0	0.882	S	78.2	112.1	0.888	S	78.2	173.4	0.893	S
98.6	33.3	0.858	BP	98.6	43.8	0.861	S	98.6	84.5	0.865	S	98.6	158.3	0.875	S	98.6	284.5	0.889	S

* BP is bubble point. DP is dew point. S is a single phase. An asterisk (*) indicates that density data were not obtained at these conditions.

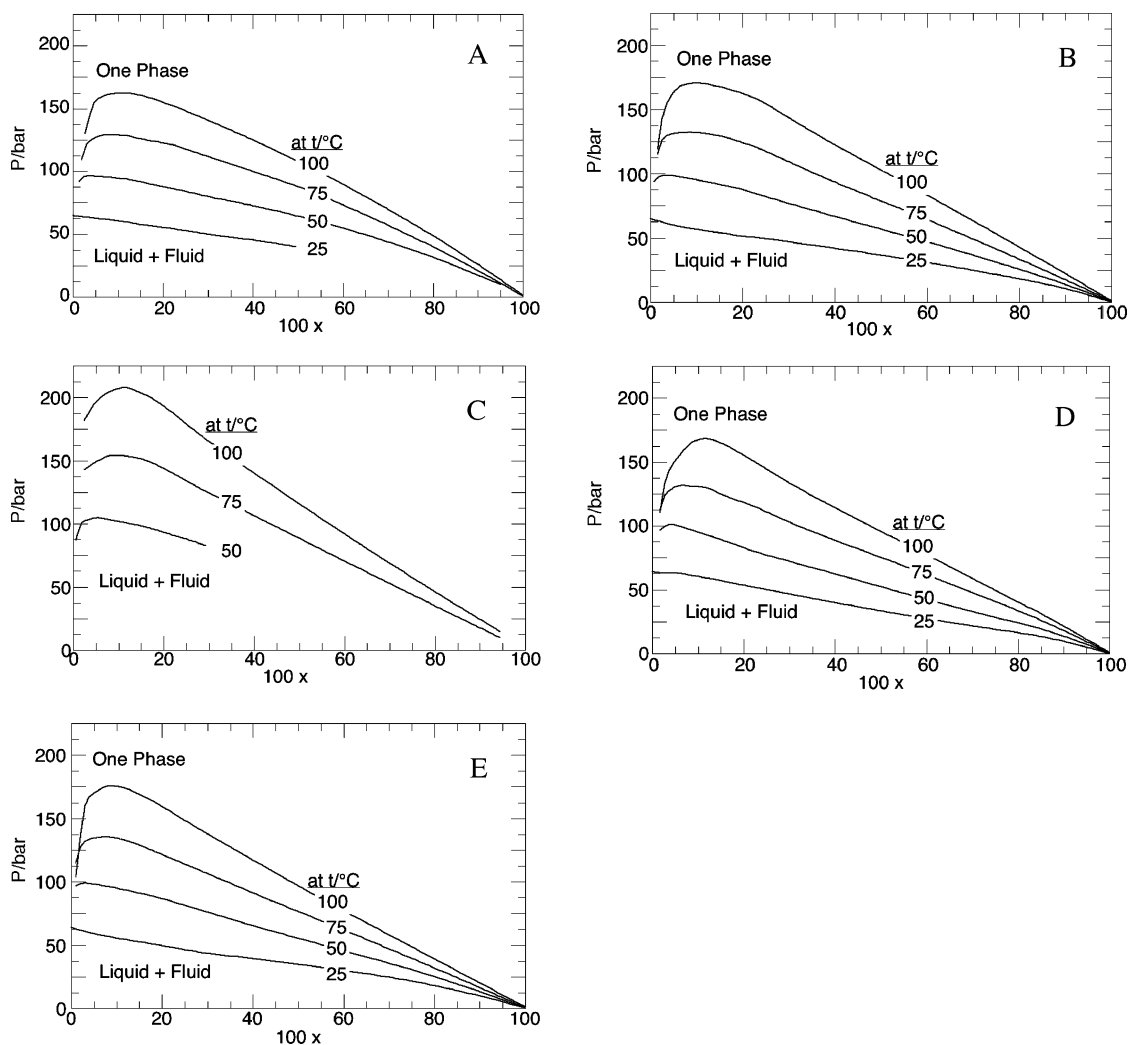


Figure 2. Isotherms for the x pyrazine + CO₂ systems obtained in this study. A, pyrazine; B, 2-methoxypyrazine; C, 2-acetylpyrazine; D, 2-methylpyrazine; E, 2,3-dimethylpyrazine. The 25 and 50 °C isotherms in panel A are truncated at the highest solute concentration investigated where the solute-rich phase was a liquid. The 50 °C isotherm in panel C is also truncated at the highest solute concentration investigated where the solute-rich phase was a liquid. The 25 °C isotherm is not shown in panel C since 2-acetylpyrazine is a solid over virtually the entire concentration range.

point curve, shifted the maximum of the isotherm to a higher pyrazine mole fraction, and caused the mixture critical pressure

to increase. In contrast, a negative value of k_{ij} decreased the mole fraction of pyrazine along the bubble point curve, shifted

Table 6 (Continued)

t	P	ρ		t	P	ρ		t	P	ρ		t	P	ρ		t	P	ρ	
°C	bar	$\text{g}\cdot\text{cm}^{-3}$		°C	bar	$\text{g}\cdot\text{cm}^{-3}$		°C	bar	$\text{g}\cdot\text{cm}^{-3}$		°C	bar	$\text{g}\cdot\text{cm}^{-3}$		°C	bar	$\text{g}\cdot\text{cm}^{-3}$	
$x = 0.565$																			
21.7	32.6	0.947	BP	21.7	70.7	0.958	S	21.7	106.2	0.961	S	21.7	152.4	0.964	S	28.6	36.6	0.920	BP
28.6	66.2	0.938	S	28.6	98.3	0.941	S	28.6	157.9	0.946	S	43.1	44.9	0.920	BP	43.1	61.7	0.923	S
43.1	100.0	0.926	S	43.1	163.8	0.935	S	56.5	53.8	0.909	BP	56.5	66.6	0.912	S	56.5	82.4	0.914	S
56.5	145.9	0.919	S	74.5	66.3	0.893	BP	74.5	82.1	0.895	S	74.5	118.3	0.901	S	74.5	185.2	0.907	S
100.4	85.2	0.865	BP	100.4	92.1	0.867	S	100.4	123.8	0.873	S	100.4	185.2	0.883	S				
$x = 0.736$																			
21.6	21.4	0.861	BP	21.6	22.4	0.861	S	21.6	38.3	0.864	S	21.6	56.9	0.864	S	44.2	30.0	0.859	BP
44.2	55.9	0.859	S	44.2	115.9	0.860	S	44.2	164.5	0.862	S	52.1	32.9	0.857	BP	52.1	61.4	0.859	S
52.1	107.2	0.860	S	52.1	181.7	0.861	S	60.8	36.2	0.854	BP	60.8	55.2	0.855	S	60.8	128.3	0.858	S
60.8	195.2	0.858	S	87.4	46.8	0.845	BP	87.4	69.7	0.846	S	87.4	111.0	0.850	S	87.4	179.7	0.853	S

^a BP is bubble point. DP is dew point. S is a single phase.

Table 7. Experimental Mixture Critical Pressure P at Temperature t for Pyrazine + CO₂ at Various Mole Fractions x of Pyrazine

x	$t/^\circ\text{C}$	P/bar
0.013	39.2	83.4
0.037	51.5	95.8
0.056	60.2	107.6
0.070	66.5	114.5

the maximum of the isotherm to a lower pyrazine mole fraction, but did not significantly change the mixture critical pressure. Rather than allow k_{ij} to vary, a value of zero is used to calculate the (100, 50, and 25) °C isotherms as shown in Figure 5. Note that the calculated isotherms are in closer agreement to experimental data at (25 and 50) °C but are in poorer agreement at 100 °C. Nevertheless, it is apparent that the PR EOS provides a reasonable estimate of the phase behavior of the pyrazine + CO₂ system with k_{ij} set equal to zero. Although not shown here, the characteristics of the calculated P , x isotherms for the

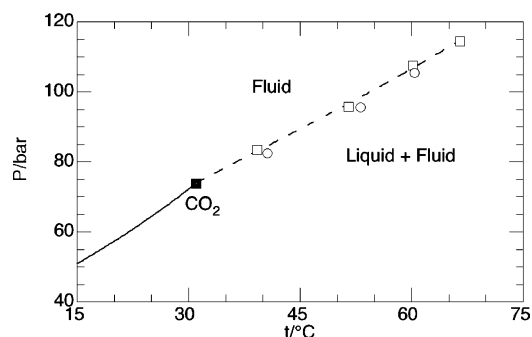


Figure 3. Comparison of a portion of the pyrazine + CO₂ mixture critical curve. □, data obtained in this study; ○, data of Yamamoto et al.;⁷ ■, critical point of pure CO₂.¹³ The dashed line is a smooth curve fit to the critical point of CO₂ and the mixture critical data obtained in this study.

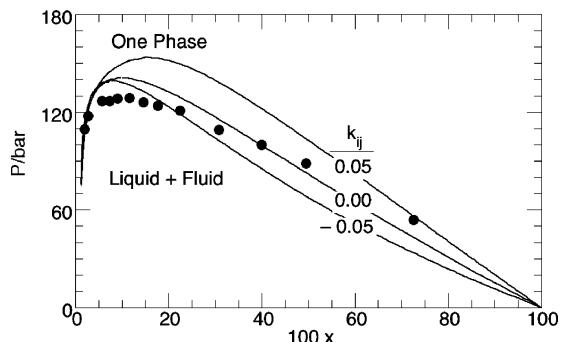


Figure 4. Effect of k_{ij} on the shape of the calculated 75 °C isotherm of the x pyrazine + CO₂ system. ●, data points obtained from a cross plot of isopleth data.

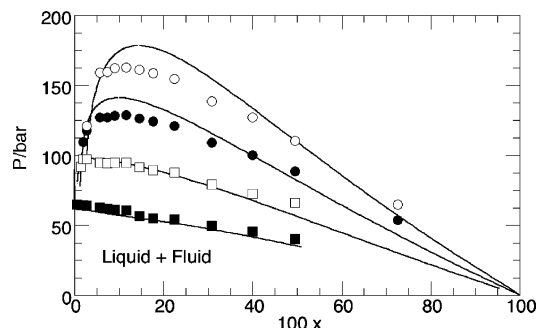


Figure 5. Comparison of calculated (lines) to experimental isotherms for the x pyrazine + CO₂ system. In this case, k_{ij} is set equal to zero. The symbols are data points obtained from a cross plot of isopleth data: ■, 25 °C; □, 50 °C; ●, 75 °C; ○, 100 °C.

2-methoxypyrazine, 2-methylpyrazine, and the 2,3-dimethylpyrazine systems are very similar to those observed with the pyrazine + CO₂ system. Once again, a zero value of k_{ij} provides a reasonable fit of the experimental data even though the critical properties of these substituted pyrazines are estimated. For 2-acetylpyrazine, the calculated 75 °C isotherm with $k_{ij} = 0$ exhibits a shape that mimics the experimental data; however, the maximum in the calculated isotherm is ≈ 75 bar higher than the observed value. A $k_{ij} = -0.100$ gave the best representation of the (75 and 100) °C isotherms, although in both cases the maximum in the calculated isotherms were $\approx (30$ to $35)$ bar too high. The poor performance of the PR EOS in this instance may be related to the high estimate of t_c for 2-acetylpyrazine.

Conclusions

Pyrazine and the substituted pyrazines considered in this study are very soluble in CO₂ at modest temperatures and pressures. The pyrazine family of compounds exhibit type-I phase behavior with CO₂, although the 2-acetylpyrazine + CO₂ system exhibits an interrupted mixture critical curve due to the appearance of solid 2-acetylpyrazine at temperatures less than 50 °C. For four of the five pyrazines considered in this study, it was possible to obtain a semi-quantitative representation of the pyrazine + CO₂ data with the PR EOS even though it is necessary to estimate the critical properties of the substituted pyrazines using the Joback–Lydersen method. The poor fit of the isotherms for the 2-acetylpyrazine + CO₂ system may be due to the very high value of the estimated critical temperature of 2-acetylpyrazine. The data presented here further substantiates the application of CO₂ as a suitable supercritical fluid solvent for extracting pyrazine compounds from natural materials.

Acknowledgment

We thank Yongchul Kim, who performed some of the experimental measurements, and we also thank Georgio Karles and Diane Gee for many helpful technical discussions concerning pyrazines. The authors are indebted to the manuscript reviewers whose technical input improved the quality of this manuscript.

Literature Cited

- (1) de Brito, E. S.; Garcia, N. H. P.; Amancio, A. C.; Valente, A. L. P.; Pini, G. F.; Augusto, F. Effect of autoclaving cocoa nibs before roasting on the precursors of the maillard reaction and pyrazines. *Int. J. Food Sci. Technol.* **2001**, *36*, 625–630.
- (2) Fadel, H. H. M.; Abdel Mageed, M. A.; Grad, A. Keeping qualities of potato chips flavoured with kebab and salt. *Nahrung-Food* **1996**, *40*, 271–273.
- (3) Hashim, P.; Selamat, J.; Muhammad, S. K. S.; Ali, A. Effect of mass and turning time on free amino acid, peptide-N, sugar and pyrazine concentration during cocoa fermentation. *J. Sci. Food Agric.* **1998**, *78*, 543–550.
- (4) Czerny, M.; Mayer, F.; Grosch, W. Sensory study on the character impact odorants of roasted arabica coffee. *J. Agric. Food Chem.* **1999**, *47*, 695–699.
- (5) King, M.-F.; Mathews, M. A.; Rule, D. C.; Field, R. A. Effect of beef packaging method on volatile compounds developed by oven roasting or microwave cooking. *J. Agric. Food Chem.* **1995**, *43*, 773–778.
- (6) Sanagi, M. M.; Hung, W. P.; Yasir, S. M. Supercritical fluid extraction of pyrazines in roasted cocoa beans effect of pod storage period. *J. Chromatogr. A* **1997**, *785*, 361–367.
- (7) Yamamoto, S.; Ohgaki, K.; Katayama, T. High-pressure phase behavior of eight binary mixtures of pyrimidine or pyrazine with CO₂, C₂H₄, C₂H₆, or CHF₃. *J. Chem. Eng. Data* **1990**, *35*, 310–314.
- (8) McHugh, M. A.; Krukonis, V. J. *Supercritical Fluid Extraction, Principles and Practice*, 2nd ed.; Butterworth-Heinenman: Boston, 1994.
- (9) Scott, R. L.; van Konynenburg, P. B. Static properties of solutions: van der Waals and related models for hydrocarbon systems. *Discuss. Faraday Soc.* **1970**, *49*, 87–97.
- (10) Nakatani, T.; Tohdo, T.; Ohgaki, K.; Katayama, T. Solubilities of pyrimidine and pyrazine derivatives in supercritical fluids. *J. Chem. Eng. Data* **1991**, *36*, 314–316.
- (11) Peng, D.-Y.; Robinson, D. B. A new two-constant equation of state. *Ind. Eng. Chem. Res. Fundam.* **1976**, *15*, 59–64.
- (12) Steele, W. V.; Chirico, R. D.; Knipmeyer, S. E.; Nguyen, A. Measurements of vapor pressure, heat capacity, and density along the saturation line for caprolactam, pyrazine, 1,2-propanediol, triethylene glycol, phenyl acetylene, and diphenyl acetylene. *J. Chem. Eng. Data* **2002**, *47*, 689–699.
- (13) Reid, R. C.; Prausnitz, J. M.; Poling, B. E. *The Properties of Gases and Liquids*; McGraw-Hill: New York, 1987.
- (14) Meilchen, M. A.; Hasch, B. M.; McHugh, M. A. Effect of copolymer composition on the phase behavior of mixtures of poly(ethylene-co-methyl acrylate) with propane and chlorodifluoromethane. *Macromolecules* **1991**, *24*, 4874–4882.
- (15) Mertdogan, C. A.; Byun, H. S.; McHugh, M. A.; Tuminello, W. H. Solubility of poly(tetrafluoroethylene-co-19 mol % hexafluoropropylene) in supercritical CO₂ and halogenated supercritical solvents. *Macromolecules* **1996**, *29*, 6548–6555.
- (16) Diguët, R.; Deul, R.; Franck, E. U. Static dielectric permittivity and density of liquid dichloromethane to 200 MPa. *Ber. Bunsen-Ges. Phys. Chem.* **1985**, *89*, 800–804.
- (17) Sen, Y. L.; Kiran, E. A new experimental system to study the temperature and pressure dependence of viscosity and density behavior of pure fluids and solutions. *J. Supercrit. Fluids* **1990**, *3*, 91.
- (18) Byun, H.-S.; DiNoia, T. P.; McHugh, M. A. High pressure densities of ethane, pentane, pentane-*d*₁₂, 25.5 wt % ethane in pentane-*d*₁₂, 2.4 wt % deuterated poly(ethylene-co-butene) (PEB) in ethane, 5.3 wt % hydrogenated PEB in pentane, 5.1 wt % hydrogenated PEB in pentane-*d*₁₂, and 4.9 wt % hydrogenated PEB in pentane-*d*₁₂ + 23.1 wt % ethane. *J. Chem. Eng. Data* **2000**, *45*, 810–814.
- (19) Hong, L.; Thies, M. C.; Enick, R. M. Global phase behavior for CO₂-philic solids: the CO₂ + β-D-maltose octaacetate system. *J. Supercrit. Fluids* **2005**, *34*, 11–16.

Received for review March 29, 2006. Accepted August 8, 2006. The authors gratefully acknowledge funding from Philip Morris USA for this project.

JE0601457